NEUROPHYSIOLOGY

Microglial pannexin-1 channel activation is a spinal determinant of joint pain

Michael Mousseau[1,2], Nicole E. Burma[1,2], Kwan Yeop Lee[3], Heather Leduc-Pessah[1,2], Charlie H. T. Kwok[1,2], Allison R. Reid[4], Melissa O'Brien[4], Boriss Sagalajev[3], Jo Anne Stratton[1], Natalya Patrick[1], Patrick L. Stemkowski[2], Jeff Biernaskie[1,5], Gerald W. Zamponi[2], Paul Salo[5], Jason J. McDougall[4], Steven A. Prescott[3,6], John R. Matyas[1], Tuan Trang[1,2]*

Chronic joint pain such as mechanical allodynia is the most debilitating symptom of arthritis, yet effective therapies are lacking. We identify the pannexin-1 (Panx1) channel as a therapeutic target for alleviating mechanical allodynia, a cardinal sign of arthritis. In rats, joint pain caused by intra-articular injection of monosodium iodoacetate (MIA) was associated with spinal adenosine 5′-triphosphate (ATP) release and a microglia-specific up-regulation of P2X7 receptors (P2X7Rs). Blockade of P2X7R or ablation of spinal microglia prevented and reversed mechanical allodynia. P2X7Rs drive Panx1 channel activation, and in rats with mechanical allodynia, Panx1 function was increased in spinal microglia. Specifically, microglial Panx1-mediated release of the proinflammatory cytokine interleukin-1β (IL-1β) induced mechanical allodynia in the MIA-injected hindlimb. Intrathecal administration of the Panx1-blocking peptide ^{10}panx suppressed the aberrant discharge of spinal laminae I-II neurons evoked by innocuous mechanical hindpaw stimulation in arthritic rats. Furthermore, mice with a microglia-specific genetic deletion of Panx1 were protected from developing mechanical allodynia. Treatment with probenecid, a clinically used broad-spectrum Panx1 blocker, resulted in a striking attenuation of MIA-induced mechanical allodynia and normalized responses in the dynamic weight-bearing test, without affecting acute nociception. Probenecid reversal of mechanical allodynia was also observed in rats 13 weeks after anterior cruciate ligament transection, a model of posttraumatic osteoarthritis. Thus, Panx1-targeted therapy is a new mechanistic approach for alleviating joint pain.

INTRODUCTION

Arthritis is the most common cause of physical disability, affecting more than 50 million adults and 300,000 children in the United States (Arthritis Foundation). In these individuals, chronic joint pain is a major clinical concern. Although peripheral pathology is a diagnostic feature of arthritis, pain correlates poorly with the extent of joint pathology, and therapies that suppress joint inflammation are often inadequate for pain control (*1*). This apparent disconnect suggests that peripheral inflammation alone does not entirely account for the pain in arthritic joints. Rather, emerging evidence indicates that joint pain is also generated and amplified by aberrant activity within nociceptive circuits of the central nervous system (CNS) (*2*). These circuits converge in the spinal dorsal horn, an area that receives, processes, and relays sensory information from primary afferent nerves originating in the joints to higher centers in the brain.

Spinal nociceptive circuits are composed of neuron-neuron and neuron-glia interactions that modulate sensory inputs from the joint. Activity from an injured joint can drive spinal microglia reactivity (*3*, *4*) and transform the output of spinal circuitry so that innocuous mechanical stimuli, such as gentle touch or normal joint rotation, elicit pain (*5*). The increased nociceptive output provides an index of central sensitization and a cellular explanation for mechanical allodynia, a key sign of arthritis in animals (*6*, *7*) and humans (*8*). In examining the interactions between the joint and spinal cord, we discovered that increased nociceptive output following joint injury critically depends on pannexin-1 (Panx1) channels expressed on microglia. Panx1 is a nonselective ion and metabolite channel unique in its ability to allow molecules <1 kDa in and out of a cell (*9*, *10*). Although recently implicated in neuropathic pain (*11*, *12*), the central mechanisms by which Panx1 contributes to joint pain remain a critical open question. Here, we show that blocking microglial Panx1 effectively alleviates joint pain in rodents. Our collective findings indicate that Panx1 is a spinal determinant of, and a therapeutic target for, chronic joint pain.

RESULTS

We induced joint injuries in adult male Sprague-Dawley rats by a unilateral intra-articular injection of monosodium iodoacetate (MIA). Rats receiving intra-articular MIA displayed marked mechanical allodynia (fig. S1, A and B) and joint pathology (fig. S1, C to E): The reduction in mechanical withdrawal threshold was observed in the ipsilateral hindpaw as early as 3 days after MIA injection and persisted at least 28 days. By contrast, intra-articular injection of saline (CTR) did not affect the mechanical threshold. Because mechanical allodynia was established by day 7 after MIA injection, subsequent behavioral and cellular experiments were performed at this time point, in which there was no discernible increase in dorsal root ganglia (DRG) expression of activating transcription factor 3 (ATF3) (fig. S2, A and B) or colony-stimulating factor 1 (CSF1) (fig. S2, C and D). In these animals, there was a marked increase in CD11b immunoreactivity (Fig. 1, A and B) and the mitotic cell marker Ki67 (fig. S3, A and B) within the spinal dorsal horn, the anatomical and cellular point of

[1]Comparative Biology and Experimental Medicine, University of Calgary, Calgary, Alberta, Canada. [2]Physiology and Pharmacology, Hotchkiss Brain Institute, University of Calgary, Calgary, Alberta, Canada. [3]Neurosciences and Mental Health, Hospital for Sick Children, Toronto, Ontario, Canada. [4]Departments of Pharmacology and Anesthesia, Pain Management and Perioperative Medicine, Dalhousie University, Halifax, Nova Scotia, Canada. [5]Department of Surgery, University of Calgary, Calgary, Alberta, Canada. [6]Department of Physiology and Institute of Biomaterials and Biomedical Engineering, University of Toronto, Toronto, Ontario, Canada.
*Corresponding author. Email: trangt@ucalgary.ca

convergence for sensory information originating from the joints. The increased Iba1 and Ki67 costaining suggests that spinal microglia are activated and proliferate in response to joint injury, and that this response coincides with mechanical allodynia. To target spinal microglia, we used intrathecal injections of the immunotoxin saporin conjugated to the Mac1 antibody (Mac1-saporin), which recognizes the Mac1 receptor found on microglia, but not neurons or astrocytes (Fig. 1C). The specific depletion of spinal lumbar microglia (fig. S3, C to G) attenuated the development of MIA-induced hypersensitivity (Fig. 1D), indicating that spinal microglia causally contribute to the development of mechanical allodynia. By contrast, intrathecal injection of nontargeting saporin control did not alter the development of MIA-induced mechanical allodynia (Fig. 1D).

Adenosine 5′-triphosphate (ATP), a key substrate released following tissue injury, critically modulates microglial activity (*13*). In response to MIA-induced joint damage, we detected elevated levels of ATP within the cerebral spinal fluid (CSF) (Fig. 1E) and increased expression of ATP-gated P2X7 receptors (P2X7Rs) on CD11b-positive cells (microglia), but not on CD11b-negative cells (neurons and astrocytes) isolated from the spinal cord (Fig. 1, F and G). To target spinal P2X7Rs, we treated rats with the selective P2X7R antagonist A740003 by either continuous intrathecal infusion (0.5 μl/hour) or a single

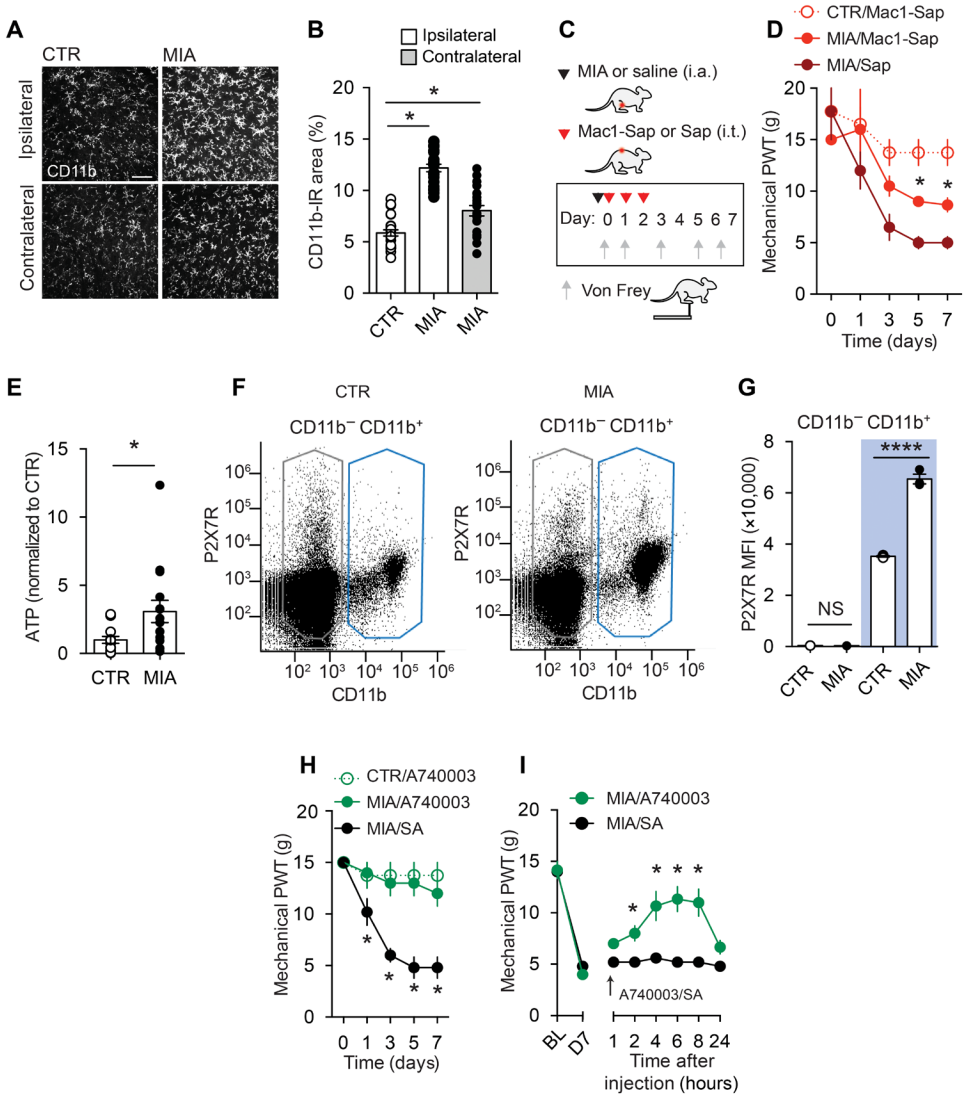

Fig. 1. Spinal microglia critically contribute to MIA-induced joint pain. (**A**) Representative images (scale bar, 100 μm) and (**B**) quantification of CD11b immunofluorescence in the L3-L5 spinal dorsal horn from MIA (2 mg) and saline CTR rats 7 days after injection (CTR/Ipsi, $n = 27$; MIA/Ipsi, $n = 21$; MIA/Contra, $n = 21$). (**C**) Schematic depicting drug administration paradigm in rats injected with intra-articular (i.a.) MIA (2 mg) or saline (CTR) and intrathecal (i.t.) Mac1-saporin (Sap; 15 μg) or saporin (15 μg). (**D**) Mechanical paw withdrawal threshold (PWT) (CTR/Mac1-Sap, $n = 4$; MIA/Mac1-Sap, $n = 6$; MIA/Sap, $n = 4$). (**E**) ATP levels in rat CSF and (**F** and **G**) flow cytometric analysis of P2X7R expression in spinal cord cell populations 7 days after injection of MIA ($n = 9$) or saline (CTR, $n = 9$). (F) Representative dot plot from CTR and MIA rats depicting gating parameters for $CD11b^-$ (black) and $Cd11b^+$ (blue) populations. (G) Histogram of P2X7R mean fluorescence intensity of $CD11b^-$ and $CD11b^+$ populations (MIA, $n = 3$; CTR, $n = 3$). NS, not significant. Effect of intrathecal A740003 on mechanical threshold following (**H**) continuous delivery [CTR/A740003, $n = 4$; MIA/A740003 10 μM, $n = 5$; MIA/saline (SA), $n = 5$] and (**I**) single injection intrathecally on day 7 (arrow) (MIA/A740003 30 μM, $n = 5$; MIA/SA, $n = 6$). $^*P < 0.05$; $^{****}P < 0.0001$, one-way analysis of variance (ANOVA) (B and G), two-way repeated-measures ANOVA (D, H, and I) followed by Sidak post hoc test, and unpaired *t* test (E).

intrathecal injection (30 μM/10 μl). Continuous pharmacological blockade of P2X7R suppressed the development of MIA-induced mechanical allodynia (Fig. 1H). In rats with established mechanical allodynia, acute intrathecal injection of A740003 produced a gradual increase in paw withdrawal thresholds that peaked at 2 hours and returned to preinjection levels by 24 hours (Fig. 1I). By contrast, intrathecal administration of the vehicle did not influence paw withdrawal thresholds (Fig. 1, H and I). Thus, P2X7R is selectively up-regulated in spinal microglia following joint injury and its activity contributes to the development and maintenance of mechanical allodynia.

Because Panx1 channel activation is a core consequence of P2X7R activity (*10*), we next examined whether joint injury affected Panx1 function in microglia. CD11b-positive cells were isolated from the spinal cord of MIA- or saline-injected rats on day 7. Panx1 function in these cells was assessed by measuring BzATP-evoked uptake of YO-PRO-1 dye, an indicator of Panx1 channel activation. Dye uptake was greater in CD11b-positive cells isolated from MIA-injected rats (Fig. 2, A and B); this response was suppressed by the Panx1-blocking peptide ^{10}panx but not by a scrambled peptide (^{scr}panx) (Fig. 2C). Spinal Panx1 contribution to MIA-induced mechanical allodynia was examined by intrathecally administering ^{10}panx. Continuous delivery of ^{10}panx prevented the development of mechanical allodynia, while an acute intrathecal injection of the Panx1-blocking peptide transiently reversed mechanical allodynia caused by intra-articular injection of MIA (Fig. 2, D and E).

To pinpoint whether Panx1 expressed specifically in microglia is required for mechanical allodynia, we generated mice with a tamoxifen-inducible deletion of *Panx1* in CX_3Cr_1-expressing cells (*Cx3cr1*-Cre^{ERT2}::*Panx1*$^{flx/flx}$) (*14*). Intra-articular injection of MIA was given 28 days after tamoxifen treatment to allow peripheral, but not central, CX_3Cr_1-expressing cells to repopulate before testing (*15*). These mutant mice, which lacked Panx1 in microglia, displayed MIA-induced spinal microgliosis and joint damage comparable to Panx1-expressing littermate control mice (vehicle-treated *Cx3cr1*-Cre^{ERT2}::*Panx1*$^{flx/flx}$) (fig. S4, A to D). By contrast, robust mechanical allodynia developed in MIA-injected Panx1-expressing mice, but not in Panx1-deficient mice (Fig. 2F), which were protected from developing mechanical allodynia for at least 28 days after MIA-induced joint damage (fig. S4E). The attenuation of mechanical allodynia was not sex-dependent (fig. S4F) or the result of tamoxifen per se, as mice lacking inducible Cre recombinase (Panx1$^{flx/flx}$) developed pain sensitivity comparable to vehicle-treated Panx1-expressing mice (fig. S4G). Together, our

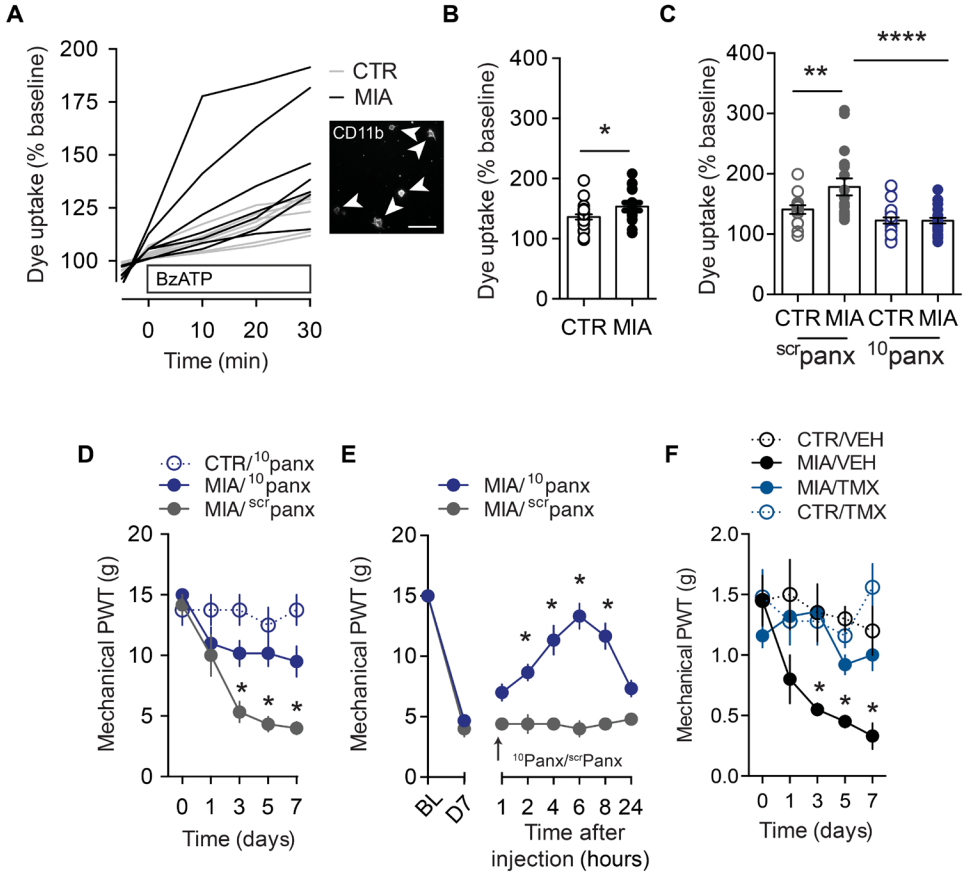

Fig. 2. Microglial Panx1 channel activation is crucial for MIA-induced mechanical allodynia. (**A**) Representative traces (scale bar, 50 μm) and (**B**) quantification of BzATP (300 μM)–evoked YO-PRO-1 dye uptake in spinal microglia isolated from adult rats 7 days after intra-articular saline (CTR, $n = 24$ cells) or MIA ($n = 18$ cells). (**C**) Effect of ^{10}panx (10 μM) and ^{scr}panx (10 μM) control peptide on dye uptake (CTR/^{scr}panx, $n = 14$ cells; CTR/^{10}panx, $n = 31$ cells; MIA/^{scr}panx, $n = 20$ cells; MIA/^{10}panx, $n = 24$ cells). (**D** and **E**) Effect of intrathecal ^{10}panx (0.5 μg/hour) or ^{scr}panx (0.5 μg/hour) on mechanical threshold following (D) continuous (CTR/^{10}panx, $n = 4$; MIA/^{10}panx, $n = 6$; MIA/^{scr}panx, $n = 6$) or (E) acute delivery on day 7 (arrow) (20 μg) (MIA/^{10}panx, $n = 6$; MIA/^{scr}panx, $n = 5$). (**F**) Mechanical threshold in vehicle (VEH) and tamoxifen (TMX) *Cx3cr1*-Cre^{ERT2}::*Panx1*$^{flx/flx}$–treated mice (CTR/VEH, $n = 4$; MIA/VEH, $n = 4$; MIA/TMX, $n = 5$; CTR/TMX, $n = 5$). *$P < 0.05$; **$P < 0.001$; ****$P < 0.0001$, unpaired *t* test (B), one-way ANOVA (C), and two-way repeated-measures ANOVA (D to F) followed by Sidak post hoc test.

findings demonstrate that Panx1 channels on microglia are required for the development of mechanical allodynia following joint injury.

In response to peripheral injury, microglia secrete various signaling molecules, one of which, interleukin-1β (IL-1β), is known to drive hyperexcitability of spinal dorsal horn neurons and contribute to arthritic pain (*16*). We confirmed in cultured BV2 microglia-like cells that BzATP induces a Panx1-dependent release of IL-1β (Fig. 3A) and, in rat CSF, that IL-1β levels are elevated 7 days after joint injury (Fig. 3B). At this time point following injury, isolation of microglia-specific transcripts from RiboTag mice (*Cx3cr1*-Cre^{ERT2}::*Rpl22*^{HA}) revealed a significant up-regulation of IL-1β mRNA in spinal microglia (Fig. 3C). The increased message was concomitant with an increase in total spinal IL-1β levels, which did not occur in microglial Panx1-deficient mice (Fig. 3D). To discern whether IL-1β contributes to mechanical allodynia, we administered IL-1β intrathecally to Panx1-deficient mice. Although these mice display attenuated mechanical allodynia after MIA injection, local delivery of recombinant IL-1β caused a progressive decrease in mechanical withdrawal threshold that was blocked by IL-1ra, a selective IL-1β receptor antagonist (Fig. 3E). Conversely, intrathecal IL-1ra delivery transiently reversed established mechanical allodynia in MIA-injected Panx1-expressing mice but did not further ameliorate mechanical allodynia in Panx1-deficient mice (Fig. 3E). These data show that IL-1β is a Panx1-dependent downstream signaling molecule released from microglia in response to joint injury and that Panx1 inhibition alleviates mechanical allodynia by abrogating the release and up-regulation of IL-1β caused by joint injury.

Mechanical allodynia is causally linked to neuronal hyperexcitability (sensitization) within spinal nociceptive circuits. We measured cFos immunoreactivity as an index of neuronal activation and determined that joint injury increased the number of cFos-positive neurons within the spinal dorsal horn of Panx1-expressing mice. By contrast, this increase in cFos immunoreactivity was absent in microglial Panx1-deficient mice (Fig. 4, A and B), which displayed attenuated mechanical allodynia (Fig. 2F). To assess neuronal function more directly, we performed extracellular single-unit recordings in vivo.

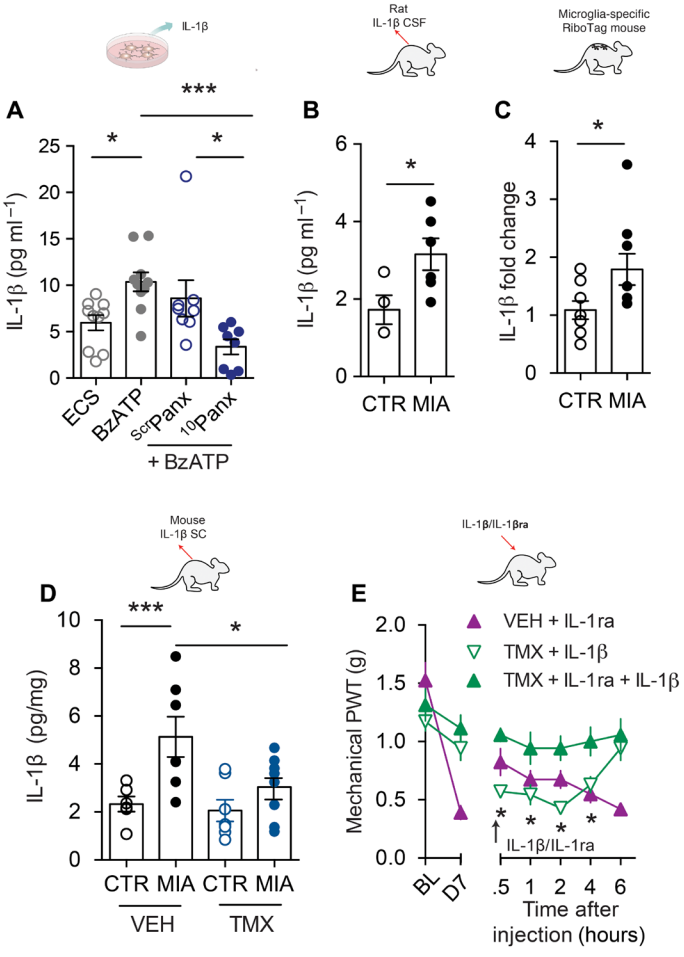

Fig. 3. Panx1-mediated IL-1β release contributes to joint pain. (**A**) IL-1β release from BV2 microglia-like cell cultures and effect of ^{10}panx (10 μM) or ^{scr}panx (10 μM) peptide (ECS, $n = 10$; BzATP, $n = 10$; ^{scr}panx, $n = 8$; ^{10}panx, $n = 8$). (**B**) IL-1β levels in rat CSF 7 days after intra-articular MIA ($n = 6$) or saline (CTR, $n = 4$) injection. (**C**) IL-1β mRNA levels of spinal microglia-specific transcripts isolated from RiboTag mice (*Cx3cr1-Cre*^{ERT}::*Rpl22*^{HA}) (MIA, $n = 9$; CTR, $n = 8$). (**D**) IL-1β levels in vehicle or tamoxifen *Cx3cr1*-Cre^{ERT2}::*Panx1*$^{flx/flx}$ mice 7 days after intra-articular MIA or saline injection (VEH/CTR, $n = 6$; VEH/MIA, $n = 7$; TMX/CTR, $n = 7$; TMX/MIA, $n = 8$). (**E**) Mechanical threshold following a single intrathecal injection on day 7 (arrow) of IL-1β (100 pg) or IL-1ra, an IL-1β receptor antagonist (50 ng), in vehicle or tamoxifen-treated *Cx3cr1*-Cre^{ERT2}::*Panx1*$^{flx/flx}$ mice (VEH/IL-1ra, $n = 8$; TMX/IL-1β, $n = 8$; TMX IL-1ra/IL-1β, $n = 7$). $^{*}P < 0.05$; $^{***}P < 0.001$, one-way ANOVA (A and D), unpaired *t* test (B and C), and two-way repeated-measures ANOVA (E) followed by Bonferroni or Sidak post hoc tests.

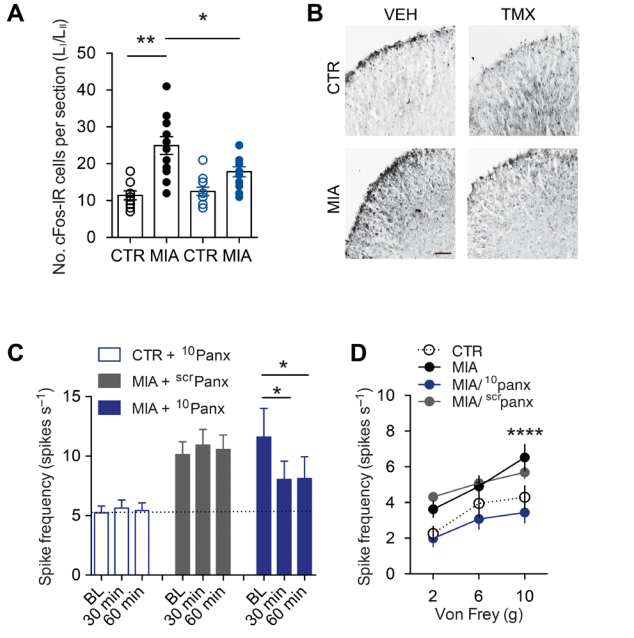

Fig. 4. Blocking Panx1 suppresses neuronal excitability in spinal L_I-L_{II} dorsal horn neurons. (**A** and **B**) Quantification and representative images of cFos immunofluorescence in the L3-L5 spinal dorsal horn from vehicle- and tamoxifen-treated *Cx3cr1*-Cre^{ERT2}::*Panx1*$^{flx/flx}$ mice after MIA or saline CTR intra-articular injection. Scale bar, 50 μm. (**C** and **D**) Rat in vivo spinal cord recordings from spinal L_I-L_{II} neurons 7 days after intra-articular MIA or saline injection. (C) Spike frequency evoked by brush (dynamic mechanical allodynia) at 30 and 60 min after ^{10}panx or ^{scr}panx peptides (CTR/^{10}panx, $n = 37$ cell recordings; MIA/^{scr}panx, $n = 22$ cell recordings; MIA/^{10}panx, $n = 29$ cell recordings). BL, baseline. (D) Stimulus-response curve showing mean response at each von Frey (static mechanical allodynia) stimulation force (MIA/^{scr}panx, $n = 20$ cell recordings; MIA/^{10}panx, $n = 27$ cell recordings; CTR/^{10}panx, $n = 20$ cell recordings). $^{*}P < 0.05$; $^{**}P < 0.01$, one-way ANOVA (A and C) and two-way repeated-measures ANOVA (D) followed by Bonferroni or Sidak post hoc tests.

The spiking of spinal laminae I-II (L_I-L_{II}) dorsal horn neurons evoked by innocuous brush or von Frey filament stimulation of the ipsilateral hindpaw (*17*) was greater in MIA-injected animals than in controls, which is consistent with mechanical allodynia. To test whether Panx1 contributed to the neuronal hyperexcitability after joint injury, we applied ^{10}panx directly onto the exposed spinal cord of animals with established mechanical allodynia. In MIA-injected rats, spinal application of ^{10}panx, but not ^{scr}panx, attenuated the spiking evoked by brush or von Frey filament stimulation (Fig. 4, C and D), indicating that Panx1 is necessary to maintain both mechanical allodynia and the hyperexcitability in spinal L_I-L_{II} neurons following joint injury. Direct application of recombinant IL-1β (5 ng) onto the spinal cord of naïve (nonarthritic) rats for 20 to 30 min increased spiking evoked by 10-g von Frey stimulation from 4.3 ± 2.9 to 8.2 ± 3.6 spike/s ($P < 0.05$, Wilcoxon signed-rank test; $n = 12$ cells) and caused a nearly significant increase in spontaneous spiking from 0.3 ± 0.2 to 2.0 ± 1.3 spike/s ($P = 0.11$, Wilcoxon signed-rank test), consistent with past studies (*16*, *18*, *19*).

Having determined that pharmacological and genetic inhibition of Panx1 ameliorates mechanical allodynia following joint injury, we sought to translate our mechanistic discovery by testing the U.S. Food and Drug Administration–approved broad-spectrum Panx1 inhibitor probenecid, an anti-gout medication (*20*). Daily systemic probenecid treatment in rats with MIA-induced joint injury prevented the progressive reduction in mechanical threshold that occurs in over 7 days (Fig. 5A) and blocked the increase in CSF IL-1β (Fig. 5B). In rats with established mechanical allodynia, a single systemic injection of probenecid transiently increased mechanical threshold (Fig. 5C) and reduced CSF levels of IL-1β (Fig. 5D) on day 7. This reversal of mechanical allodynia was also observed on days 14 (fig. S5A) and 28 (fig. S4E) after MIA-induced joint injury. To further investigate the impact of probenecid on nociceptive threshold, we used dynamic weight-bearing asymmetry to evaluate spontaneous pain. Specifically, at 7 and 14 days after intra-articular MIA injection, rats displayed significant weight-bearing asymmetry, as evidenced by reduced weight bearing (load) on the ipsilateral hindlimb compared to the nonaffected hindlimb (fig. S5B). The change in weight distribution was accompanied by a decrease in paw surface distribution, consistent with guarding of the MIA-injected limb (fig. S5C). Systemic administration of probenecid on days 7 (Fig. 5, E and F) and 14 (fig. S5, D and E) significantly improved both weight-bearing and paw surface distribution in MIA-injected rats. We next examined whether probenecid affected peripheral nociceptive inputs from the joint by performing in vivo extracellular recordings of rat knee joint Aδ and C afferent nerve fibers. In this preparation, noxious rotation of the MIA-injected knee elicited action potentials that were greater in frequency than those recorded in saline-injected sham controls (fig. S6, A to C). However, joint afferent firing in MIA- or saline-injected rats was not diminished by systemic probenecid treatment, indicating that the actions of probenecid were not due to inhibition of peripheral afferent activity, pointing instead to centrally mediated effects.

The potential clinical utility of probenecid was further validated in a chronic joint injury model induced by transection of the anterior cruciate ligament (ACL) (Fig. 6A) (*21*). The chronicity of joint pathology and the onset of joint pain following ACL transection (ACLx) recapitulate key features in the progression of posttraumatic osteoarthritis (OA) in humans (*22*). In mice, mechanical allodynia developed approximately 6 to 8 weeks following ACLx and persisted up to at least week 13 (fig. S7, A and B). At this later time point, systemic

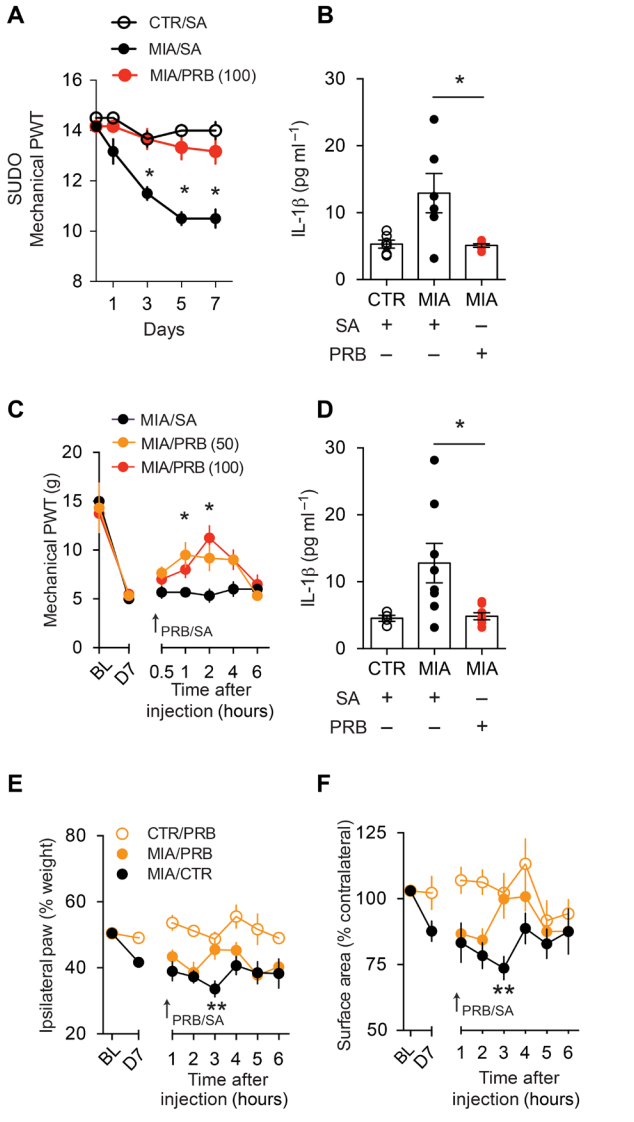

Fig. 5. Treatment with probenecid, a broad-spectrum Panx1 blocker, alleviates MIA-induced pain behaviors. (**A**) Mechanical paw withdrawal threshold assessed by von Frey filaments using the SUDO method in rats injected twice daily intraperitoneally with probenecid (PRB) or saline [CTR/SA, $n = 6$; MIA/SA, $n = 6$; MIA/PRB (100 mg/kg), $n = 6$]. Baseline threshold in gram force: 14.5 g. (**B**) IL-1β levels in rat CSF 7 days after intra-articular MIA/CTR and daily intraperitoneal injection of saline or probenecid (CTR/SA, $n = 6$; MIA/SA, $n = 6$; MIA/PRB 100 mg/kg, $n = 6$). (**C**) Mechanical paw withdrawal threshold assessed by von Frey filament test on day 7 after MIA-induced joint injury (saline, $n = 6$; probenecid 50 mg/kg, $n = 6$; probenecid 100 mg/kg, $n = 4$). (**D**) IL-1β levels in rat CSF 7 days after intra-articular MIA/CTR and acute intraperitoneal injection of saline or probenecid (CTR/SA, $n = 4$; MIA/SA, $n = 8$; MIA/PRB 100 mg/kg, $n = 8$). (**E** and **F**) Dynamic weight bearing assessed on day 7 after MIA-induced joint injury (CTR/PRB, $n = 8$; MIA/PRB, $n = 7$; MIA/SA, $n = 8$). Effect of probenecid (50 mg/kg) on (E) weight bearing (day 7; $P = 0.0036$, two-way ANOVA) and (F) paw surface area (day 7; $P = 0.05$, two-way ANOVA). Arrow represents single intraperitoneal injection of probenecid. *$P < 0.05$; **$P < 0.01$, two-way repeated-measures ANOVA (A, C, E, and F) and one-way ANOVA (B and D) followed by Sidak or Bonferroni post hoc tests.

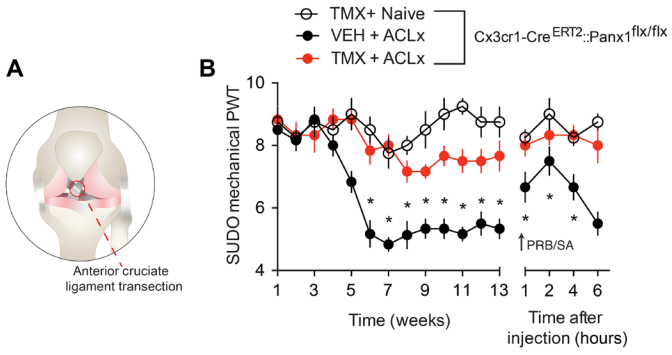

Fig. 6. Probenecid alleviates ACLx-induced joint pain. (**A**) Illustration depicting an ACLx. (**B**) Mechanical paw withdrawal threshold measured in vehicle- and tamoxifen-treated *Cx3cr1*-Cre^{ERT2}::*Panx1*$^{flx/flx}$ mice up to 13 weeks after ACLx surgery (Naive, $n = 4$; VEH/ACLx, $n = 6$; TMX/ACLx, $n = 6$). Mechanical paw withdrawal threshold following single injection of probenecid (100 mg/kg intraperitoneally; arrow) 13 weeks after surgery. Mechanical paw withdrawal threshold in mice was assessed by von Frey filaments using the SUDO method. Baseline threshold in gram force: 1.1 g. *$P < 0.05$, two-way repeated-measures ANOVA (B) followed by Sidak post hoc test.

probenecid (100 mg/kg) injection rapidly and transiently reversed mechanical allodynia (fig. S7B). Notably, microglial Panx1-deficient mice were protected from developing mechanical allodynia, and systemic injection of probenecid had no impact on mechanical threshold (Fig. 6B). Thus, a common microglial Panx1-dependent mechanism underlies both MIA- and ACLx-induced arthralgia. Our findings open the possibility that probenecid, and other clinically available broad-spectrum Panx1 inhibitors, may be used in the treatment of joint pain.

DISCUSSION

The present study demonstrates that Panx1 channels expressed on microglia are critically required for mechanical allodynia after joint injury. Pharmacological blockade or genetic deletion of microglial Panx1 effectively alleviated mechanical allodynia and blunted IL-1β release. We provide proof of concept for the potential translation of Panx1-targeted therapies by demonstrating the potent reversal of mechanical allodynia with probenecid, a clinically approved broad-spectrum Panx1 blocker. The striking reduction in pain behavior by probenecid was demonstrated several weeks after MIA-induced joint injury and months after chronic posttraumatic OA induced by ACLx. Together, our results indicate that Panx1 channel activation is a spinal determinant of chronic joint pain. Panx1 is therefore a novel and promising therapeutic target for treating joint pain.

Intra-articular injection of MIA is a robust preclinical model of arthralgia because it produces well-characterized joint pathology associated with a distinct pain phenotype. In rats and mice, MIA-induced joint injury was concomitant with the development of mechanical allodynia and increased microglial reactivity in the L3-L4 spinal dorsal horn, where the vast majority of sensory information from neurons innervating the rat knee joint is received (*23*). Injury induced changes in the firing properties of these articular afferents, increasing their response to noxious joint rotation and innocuous mechanical input, as well as generating spontaneous bursts of activity (*24*). This increased peripheral afferent drive observed in MIA-injured rats undoubtedly underlies signs of joint pain and may also trigger the spinal microglia response to injury. To engage microglia, injured sensory afferents that terminate in the spinal dorsal horn secrete a variety of molecules, with spinal ATP release being a key substrate for microglia activation and the development of pain hypersensitivity (*13*). In rats with MIA-induced joint damage, we found that increased levels of ATP within the CSF were accompanied by enhanced expression of ATP-gated P2X7Rs on spinal microglia. Increased P2X7R expression is a distinct feature of reactive microglia that does not occur in neurons or astrocytes in the spinal cord. The possible sources of ATP required to activate P2X7R and cause mechanical allodynia could include injured joint afferent terminals, spinal dorsal horn neurons, microglia, and astrocytes (*13*).

The localization of P2X7R on microglia and identification of P2X7R as a therapeutic intervention in a variety of chronic pain conditions provide the impetus for developing highly selective P2X7R antagonists (*25*). Despite advancing our understanding of P2X7R function, the clinical translation of these antagonists has been hampered by concerns about toxicity and lack of penetration into the CNS (*25*–*27*). Our study establishes Panx1 as an alternative target within the P2X7R pathway, positioning P2X7R as an upstream signaling node through which joint injury augments Panx1 function in spinal microglia. By blocking spinal Panx1, we provide the initial evidence implicating spinal Panx1 in both the development of joint pain and the maintenance of this pain after it has been established.

One of the key mechanisms for the chronicity of pain in arthritis is sensitization of nociceptive circuits (*28*). We show that joint injury by intra-articular injection of MIA changed the output of L_I-L_{II} spinal dorsal horn neurons, causing them to respond to innocuous mechanical stimuli. L_I comprises one of the principal output pathways responsible for transmitting nociceptive information from the spinal cord to the brain, and L_{II} comprises a complex network of excitatory and inhibitory interneurons that control the flow of information through L_I (*29*). The exaggerated neuronal responses after joint injury were reversed when ^{10}panx was applied locally onto the spinal cord of MIA-injured rats, suggesting that Panx1 activity is necessary to sustain aberrant spinal nociceptive output after joint injury. It is important to consider that Panx1 channels are also expressed on dorsal horn neurons (*30*), and therefore, the reversal of mechanical sensitivity by ^{10}panx may not be mediated solely via microglial Panx1.

To discern the role of microglial and neuronal Panx1, we created mice in which Panx1 was deleted, in a tamoxifen-dependent manner, in CX_3Cr_1-positive cells. Central and peripheral CX_3Cr_1-expressing cells have different rates of cell turnover: Microglia are self-renewing with a low turnover rate (*31*), while peripheral monocytes and macrophages rapidly turn over and are replenished by bone marrow precursor cells (*32*). Cre-dependent recombination in microglia persists for at least 4 weeks after tamoxifen treatment, whereas peripheral CX_3Cr_1-expressing cells that underwent recombination are replaced by nonrecombined CX_3Cr_1-expressing cells (*15*). To allow peripheral CX_3Cr_1-expressing cells to repopulate, joint injury was induced approximately 4 weeks after tamoxifen treatment. These mice therefore lacked Panx1 only in microglia and were protected from MIA-induced mechanical allodynia but still developed significant peripheral joint pathology. In addition, we observed no appreciable change in neuronal activation, as measured by cFos immunoreactivity, in our transgenic mice after intra-articular injections of MIA. Thus, Panx1 expressed

centrally on microglia, and not on neurons or peripheral CX_3Cr_1-expressing monocytes, is critically required for the development of joint pain.

Although peripheral immune cells have known roles in joint damage, it remains to be determined whether Panx1 on peripheral CX_3Cr_1-expressing cells contributes to the progression of joint pathology. Cross-talk between the arthritic joint and CNS, however, can be instigated by the release of proinflammatory cytokines, such as IL-1β (*33*). The actions of IL-1β are not restricted to the periphery, with several studies reporting a concomitant increase in spinal IL-1β expression and nociceptive behaviors following joint injury (*33*, *34*). Here, we found that MIA-induced joint damage was associated with elevated CSF levels of IL-1β. While an increase in IL-1β has been reported in the CSF of rheumatoid arthritis patients (*33*), it remains unclear how joint injury might increase IL-1β levels in the CNS. One possibility is that circulating IL-1β may enter the CNS by direct passage through areas of the blood-brain barrier that are more permeable (*35*). It is also possible that peripheral cytokines sensitize articular afferents, which, in turn, provide the aberrant nociceptive input that somehow drives cytokine release in the CNS. Microglia are a prominent source of IL-1β in the spinal cord (*36*), but the release of this cytokine in response to joint injury can come from a variety of other cells, including astrocytes and neurons (*34*). We show that spinal microglia up-regulate IL-1β mRNA expression in response to joint injury, with Panx1 activation being a requisite step that drives the release of IL-1β from microglia. Furthermore, intrathecal administration of IL-1β reinstated a robust pain phenotype in microglial Panx1-deficient mice, which otherwise were protected from developing MIA-induced mechanical allodynia. Our results reveal a missing spinal mechanism linking joint injury and afferent sensitization to spinal microglial Panx1 activation and IL-1β release in the pathogenesis of chronic joint pain. By positioning Panx1 as a critical target upstream of IL-1β release, we highlight the potential for blocking Panx1 as a new avenue for treating joint pain.

IL-1β is an important target of biologics used to treat a variety of arthritides (*16*). These biological drugs suppress joint inflammation through a peripheral mechanism of action, yet pain remains a major problem in individuals with arthritis (*37*). Our findings provide an unexpected therapeutic option: probenecid, a clinically used broad-spectrum Panx1 inhibitor that blocks IL-1β release (*20*, *38*, *39*). Systemic administration of probenecid reversed mechanical allodynia several weeks after MIA-induced joint injury and in animals with chronic OA caused by ACLx. The striking reversal by a single injection of probenecid implies that ongoing Panx1 activity is required to sustain pain hypersensitivity. As probenecid did not alter peripheral afferent activity in the injured joint, these findings suggest a central mechanism of action rather than direct inhibition of peripheral nociceptive input (*40*). Notably, inhibition of Panx1 by probenecid, ^{10}panx, or genetic ablation suppressed pain behaviors without affecting acute nociception. Thus, Panx1-targeted therapies would not be expected to impair normal pain sensitivity, which is protective and warns of potential injury. Genetic or pharmacological blockade of Panx1 also had no impact on P2X7R cation channel function (*14*), making it possible to differentially target Panx1 and avoid adverse effects associated with P2X7R-based therapies.

In summary, we show that Panx1-mediated IL-1β release from microglia is a spinal determinant of joint pain. Drug development for centrally mediated pain has mainly focused on blocking P2X7R (*25*, *41*), which we have determined is an upstream signaling node through which joint injury drives Panx1 activation. Thus, blocking Panx1 while leaving P2X7R cation channel function intact could be a promising adjuvant therapy or alternate strategy for alleviating joint pain. The availability of clinically approved Panx1-blocking drugs, such as probenecid, paves the way for direct therapeutic translation of even more selective and potent Panx1-targeted therapies as treatments of arthritis joint pain.

METHODS

Study approval

Some of the methods described below are similar to methods used in earlier research (*17*). All experiments were approved by the University of Calgary, Hospital for Sick Children, and Dalhousie University Animal Care Committees, and all animals were under veterinary supervision in accordance with the Canadian Council on Animal Care.

Statistics

Data were presented as means ± SEM and analyzed using GraphPad Prism 6 software by unpaired *t* test (two-sided) or one-way ANOVA with Bonferroni or Sidak post hoc test. Time course and daily behavior were analyzed using two-way repeated-measures ANOVA with Sidak post hoc tests. $P < 0.05$ was considered significant.

Animals

Male Sprague-Dawley rats (age 8 to 12 weeks; Charles River Laboratories) and mice (background C57BL6/J, *Cx3cr1*-Cre^{ERT2}::*Panx1*$^{flx/flx}$, and *Cx3cr1*-Cre^{ERT}::*Rpl22*^{HA}, age 8 to 12 weeks) were housed under a 12-hour light/dark cycle with ad libitum access to food and water.

Intra-articular injection of MIA

Joint pathology was induced in anesthetized rodents (isoflurane, 2 to 3% in 100% oxygen) by an intra-articular injection of MIA (Sigma) into the knee joint flexed at a 90° angle: 25 μl of MIA (80 mg/ml) in sterile saline (0.9%) was injected into the right (ipsilateral) knee of the rat with a 30-gauge needle. Mice were injected with 10 μl of MIA (10 mg/ml) in sterile saline (0.9%) in the right knee. Control rats and mice received an intra-articular injection of 25 or 10 μl of sterile saline.

Nociceptive behavioral test

Mechanical allodynia was assessed by measuring the hindpaw withdrawal threshold to von Frey filaments. Briefly, animals were placed in Plexiglas boxes on a grid surface through which von Frey calibrated filaments (IITC) could be applied. Both mice and rats were habituated for 1 hour 1 day before baseline behavior and 30 min before baseline testing. Von Frey filaments were applied to the central region of the plantar surface beginning with the lowest hair (mice, 0.16 g; rats, 2 g). A trial consisted of three to five applications of the filament to the hindpaw (maintained for approximately 2 s) at 30-s intervals. If withdrawal did not occur during the three applications of a particular hair, then the next largest hair in the series was applied. When the hindpaw was withdrawn from a particular hair three times of five applications, the value of that hair in grams was considered to be the withdrawal threshold (*42*). The baseline withdrawal thresholds were determined for each animal before MIA injection (day 0). Measurement of paw withdrawal threshold was measured up to 28 days. In a subset of experiments (day 28; *Cx3cr1*-Cre^{ERT2}::*Panx1*$^{flx/flx}$ mice), the simplified up-down (SUDO) method with von Frey filaments was used for measuring mechanical threshold in rodents; values are represented as paw

withdrawal threshold integer values (*43*). Behavioral tests were conducted with the experimenter blinded to genotype and/or treatment.

Knee histopathology and scoring

Mice and rats were anesthetized with pentobarbital and perfused transcardially with phosphate-buffered saline (PBS) and then 10% neutral buffered formalin (NBF). The hind knees were dissected 7 days after intra-articular MIA or saline injection and postfixed for 3 to 5 days in 10% NBF. After fixation, the knees were decalcified in 10% EDTA/double-distilled water (pH 7.4) for 3 weeks at room temperature. Solution was changed daily for the first week and once per week following. The knees were split in the sagittal plane and embedded in paraffin using a Leica automatic tissue processor. Serial sagittal sections of the knees were cut at 8 μm on a microtome (Leica) and stained with safranin O or hematoxylin and eosin. Knee joint histopathology was graded by two independent evaluators blinded to the treatment conditions, using the modified Mankin (*44*) and Osteoarthritis Research Society International (OARSI) scoring systems (*45*). The modified Mankin scoring system assessed four categories of OA features: articular structure, cellularity, cartilage staining, and tidemark. The structure was assessed on a scale of 0 to 6 (0, normal; 1, irregular surfaces; 2, pannus; 3, cleft to transitional zone; 4, clefts to radial zone; 5, clefts to calcified zone; 6, complete disorganization). The appearance of articular cells was scored on a scale of 0 to 3 (0, normal; 1, diffuse hypercellularity; 2, clusters; 3, hypocellularity). Matrix staining was scored on a scale of 0 to 4 (0, normal; 1, slight reduction; 2, moderate reduction; 3, severe reduction; 4, no dye noted), and the tidemark was scored as 0 or 1 (0, intact; 1, crossed by blood vessels). The total Mankin score was established by adding the scores of all four assessments. The OARSI scoring system assessed the grade and stage of the affected articular cartilage. Knee joint pathology was graded on a scale of 0 to 6.5 (0, uninvolved; 1, cells intact; 1.5, cell death; 2, fibrillation through superficial zone; 2.5, abrasion matrix loss through superficial zone; 3, simple fissures; 3.5, branched fissures; 4, surface delamination; 4.5, mid-zone evacuation; 5, bone surface intact; 5.5, reparative tissue present; 6.0, marginal osteophytes; 6.5, marginal and central osteophytes). Staging was assessed on a scale of 0 to 4 for OA activity seen in knee joint (0, no OA; 1, <10%; 2, 10 to 25%; 3, 25 to 50%; 4, >50%). The grade and stage were added for a total OARSI score.

Intrathecal drug administration

Rats received intrathecal drug delivery by micro-osmotic pump implantation (Alzet). Rats were anesthetized with isoflurane (2% in 100% oxygen), and a catheter connected to an osmotic pump was surgically inserted into the intrathecal space of the lumbar (L3-L5) segment of the spinal cord. Osmotic pumps administered continuous drug delivery (0.5 μl/hour) for 7 days during the development of MIA-induced joint pain. In a subset of experiments, both rats and mice, 7 days after MIA injection, were subject to intrathecal drug administration under isoflurane anesthesia by lumbar puncture, as previously described (*46*). Drugs administered to the intrathecal space in rats included the following: P2X7R antagonist A740003 (10 μM delivered 0.5 μl/hour; 10 μl of 30 μM acute intrathecally) (Sigma-Aldrich), mimetic peptide inhibitor of Panx1, ^{10}panx (sequence: WRQAAFVDSY) and ^{scr}panx (sequence: FSVYWAQADR) (0.5 μg/hour in mini-osmotic pump; 20 μg acute intrathecal sequence) (New England Peptide), and Mac1-saporin and saporin (15 μg per intrathecal injection on days 0, 1, and 2; Advanced Targeting Systems). In a subset of experiments, mice received intrathecal drug administration without isoflurane. Mice received 5 μl of IL-1ra (0.01 μg/μl; R&D Systems) and/or 5 μl of the IL-1β recombinant protein (20 pg/μl; R&D Systems) before behavioral assessment. Control animals received equivalent volume of 0.9% saline.

Immunohistochemistry

Rats and mice were anesthetized with pentobarbital (Bimeda-MTC Animal Health Inc.) and perfused transcardially with PBS and then 4% (w/v) paraformaldehyde (PFA) in 0.1 M phosphate buffer (pH 7.4). The lumbar segment of the spinal cord was dissected and postfixed overnight in 4% PFA. The spinal cord was cryopreserved in 30% sucrose and embedded in OCT (optimal cutting temperature) compound. The L3-L5 lumbar segment of the spinal cord was sectioned at 30 μm using a cryomicrotome; free-floating sections were incubated overnight at 4°C in mouse anti-CD11b (1:50, CBL1512, EMD Millipore), rat anti-CD11b (1:500, ab64347, Abcam), mouse anti-PU.1 (1:500, 149819, Invitrogen), mouse anti-Ki67 (1:500, 14569881, Invitrogen), and rabbit anti-Iba1 (1:500, 01919741, Wako) in PBS. Sections were washed and incubated at 4°C with fluorochrome-conjugated secondary antibodies [1:1000, Cy3-conjugated affiniPure donkey anti-mouse immunoglobulin G (IgG), Jackson ImmunoResearch, or Cy5-conjugated donkey anti-rabbit IgG, Jackson ImmunoResearch]. Images were obtained using a Nikon Eclipse Ti C1SI spectral confocal microscope and a Nikon A1R multiphoton microscope. The images were converted using NIS-Elements imaging software (Nikon), and quantification of images was performed using ImageJ [National Institutes of Health (NIH)], with the experimenter blinded to genotype and/or treatment.

Isolation of mixed spinal cord neuron-glia cultures for flow cytometry and YO-PRO-1 dye uptake

Mixed neuron-glia cultures were acutely isolated from the adult rat spinal cord from both MIA-injected and saline control animals 7 days after MIA injection. Rats were anesthetized with pentobarbital and perfused transcardially with PBS. Spinal cords were rapidly isolated by hydraulic extrusion into Hanks' balanced salt solution. The lumbar spinal cord contents were dissociated and filtered through a 70-μm cell strainer into Dulbecco's modified Eagle's medium (DMEM) containing 10 mM Hepes and 2% fetal bovine serum (FBS). The cell suspension was combined with isotonic Percoll (D = 1.23 g/ml) (GE Healthcare) followed by underlay of Percoll (1.08 g/ml) and centrifuged at 3000 rpm for 30 min at 20°C. The myelin debris was removed, and the interface between the Percoll gradients was collected into fresh medium and centrifuged at 1350 rpm for 10 min at 4°C. The pellet was resuspended in 10% FBS in PBS blocking solution. Cells were stained with fluorophore-conjugated antibodies P2X7R-ATTO 633 (1:250, Alomone) and CD11b/c-phycoerythrin (PE) (1:500, eBioscience) for 45 min at 22°C. Fluorescence was measured by an Attune acoustic focusing cytometer (Applied Biosystems). Live single-cell populations were gated using forward and side scatterplots. CD11b- and P2X7R-positive staining was gated using BL2 and RL1 intensities, respectively, and compared to unstained control cells. To assess Panx1 function in adult microglia, neuron-glia cultures were isolated, as reported above, from adult male rats 7 days after MIA or saline intra-articular injection. The cells were plated in DMEM containing 10% FBS and 1% penicillin-streptomycin and incubated overnight at 37°C with 5% CO_2. Cells were washed and incubated with CD11b/c-PE (1:500) and YO-PRO-1 dye (2.5 μM, Invitrogen) (dye fluorescent emission, 491/509 nm) in extracellular solution (ECS) containing 140 mM NaCl, 5.4 mM KCl, 1.3 mM $CaCl_2$, 10 mM Hepes, and 33 mM glucose (pH 7.35; osmolarity,

315 mOsm). Drugs used in this study included ^{10}panx (10 μM) and ^{scr}panx (10 μM). Drugs were incubated for 10 min before BzATP stimulation. Microglia were identified from mixed cultures by CD11b/c-PE stain. The baseline fluorescence of individual microglia was recorded for 5 min and then for 30 min after BzATP stimulation (300 μM). Fluorescence at 30 min was expressed as percentage change from baseline recorded from the same cell. All experiments were conducted at room temperature using an inverted microscope (Nikon Eclipse Ti C1SI Spectral Confocal), and the fluorescence of individual microglia was recorded using EasyRatioPro software (PTI).

cFos immunolabeling

Mouse spinal cords were isolated, and the lumbar segment (L3-L5) was sectioned, as described above. Free-floating sections were blocked first for 10 min in 0.3% H_2O_2 and then for 5 min in $NaBH_4$. The sections were incubated overnight in rabbit anti-cFos (1:5000, ab7963, Abcam) at 4°C. The sections were washed in PBS and placed in biotinylated anti-rabbit secondary antibody (1:1000, Vector Laboratories Inc.) for 2 hours at room temperature. The sections were then processed with a Vectastain ABC kit (Vector Laboratories Inc.) and developed for 45 s using 3,3-diaminobenzidine with nickel. Images of the spinal cord sections were taken with Olympus Virtual Slide System Macro Slide Scanner. cFos counts in the superficial spinal dorsal horn (up to a depth of 125 μm) were counted by an experimenter blinded to genotype and/or treatment.

CSF extraction and ATP/IL-1β measurement

CSF was obtained from the rats, as previously reported by Pegg *et al.* (*47*). Briefly, rats were anesthetized with 2% (v/v) isoflurane and placed in a stereotaxic device (Kopf Instruments). The head and neck were shaved, and a midline incision was made to expose the cisterna magna and the area blotted dry of blood. Using pulled capillary tubing, a tube was inserted through the dura mater at a parallel angle to collect CSF. CSF volume ranged from 75 to 150 μl and was stored in a 0.5-ml tube at −80°C with 1 μM ARL67156 (Sigma) to minimize ATP degradation. Samples contaminated with blood were not included in this study. ATP levels were detected using an ATP Determination kit (Life Technologies). The samples were combined with firefly luciferase and its substrate D-luciferin. Using bioluminescence, the ATP concentration was detected using a FilterMax F5 place reader at 27°C. The relative concentration of IL-1β in rat CSF was measured using antibody-based multiplex immunoassays (Luminex, Eve Technologies).

Generation of *Cx3cr1*-Cre^{ERT2}::*Panx1*$^{flx/flx}$ mice

Panx1 was floxed specifically from microglia using a Cre-loxP system. Panx1$^{flx/flx}$ mice were provided by R. Thompson (*48*), in which the flox sequence flanked exon 2 of the *Panx1* gene. These mice were crossed with C57BL6/J mice expressing Cre-ER and enhanced yellow fluorescent protein (eYFP) under control of the CX_3CR_1 promoter [JAX mice, B6.129P2(Cg)-Cx3cr1$^{tm2.1(cre/ERT)Litt}$/WganJ; stock number, 021160] and backcrossed eight generations to yield conditional knockout *Cx3cr1*-Cre^{ERT2}::*Panx1*$^{flx/flx}$ mice. Intraperitoneal injection of 1 mg of tamoxifen (Sigma) for 5 days was used to induce Cre recombination. Wild-type mice were littermates and received vehicle injections (sunflower oil with 10% ethanol) for 5 days. To control for tamoxifen effects, $CX_3CR_1^{-/-}$Panx1$^{flx/flx}$ littermates received 5 days of tamoxifen injections. Baseline behavior and MIA injection occurred 28 days following final tamoxifen injection.

Spinal cord electrophysiology

Rats were anesthetized using urethane (20% in normal saline; 1.2 g/kg intraperitoneally). A laminectomy was performed to expose the L4-S1 segments of the spinal cord. The rat was then transferred to a stereotaxic frame, and its vertebrae were clamped above and below the recording site to immobilize the spinal cord. The left hindpaw was immobilized in plasticine, with the plantar surface facing upward for stimulation. Rectal temperature was kept at 37°C using a feedback-controlled heating pad (TR-200, Fine Science Tools) throughout the experiment. To target drug delivery to the recording site, a well was built around the recording site using petroleum jelly. A four-electrode array with a total of 16 recording sites (A4 type, NeuroNexus) was then implanted at the L5 spinal level. The array was oriented so that each electrode was at the same mediolateral position. The depth of electrode insertion below the dorsal surface was monitored. Because recording sites are spaced at 50-μm intervals up each electrode, we determined on which site a unit was recorded and, from this, measured the depth of recorded neurons. Brush stimulation was applied to the hindpaw to identify neurons responsive to low-threshold mechanical input. The signal was amplified, band-pass–filtered between 500 Hz and 10 kHz, digitized at 20 kHz with an OmniPlex data acquisition system (Plexon), and stored with stimulus markers on disk. Single units were isolated using Offline Sorter V3 software (Plexon) and analyzed with NeuroExplorer 4 (Plexon).

Systemic drug administration

In a subset of experiments, probenecid (50 and 100 mg/kg, Life Technologies) was dissolved in saline at a concentration of 15 or 30 mg/500 μl and administered in a volume of 500 μl/300 g body weight. To examine the effect of nonselectively blocking Panx1 on the development of joint pain, daily probenecid injections (100 mg/kg per intraperitoneal injection) were administered twice a day for 7 days after intra-articular MIA injection. In a separate cohort, a single injection of probenecid (100 mg/kg intraperitoneally) was administered in animals with established MIA-induced mechanical allodynia. Control animals received an equivalent volume of saline.

Dynamic weight bearing

The distribution of weight borne on the hindlimbs was measured using a dynamic weight bearing system (Bioseb). Animals were placed in a Plexiglas chamber (24 cm long × 24 cm wide × 30 cm tall) and allowed to move freely. The animals were tested on day 0 (baseline), day 7, and day 14 after MIA injections. The floor of the chamber has a sensor array that measures the position, surface area, and level of applied pressure (weight). A camera was mounted at the top of the chamber to record the animal's movements. The sensor data and camera footage were analyzed together to calculate the weight applied by each of the animal's limbs and the surface area of the paws in contact with the walking surface over a 3-min recording period. On test day, baseline was measured, then animals were given an intraperitoneal injection of either saline or probenecid, and incapacitance was assessed every hour for 6 hours.

Peripheral afferent electrophysiology

Animals were anesthetized with urethane (25% stock solution; 2 g/kg intraperitoneally) and artificially ventilated with 100% O_2 (Harvard Apparatus). The muscle relaxant gallamine triethiodide (50 mg/kg intravenously) was administered, which eliminated neural interference from hindlimb musculature, and the saphenous nerve was isolated

and transected in the inguinal region to prevent spinal reflexes. Fine neurofilaments were teased from the saphenous nerve and placed over a platinum recording electrode for subsequent recording. The mechanosensitivity of Aδ and C joint afferent fibers was assessed by rotating the knee joint by a fixed level of torque that was in the noxious range. After three baseline rotations, probenecid (50 mg/kg) or vehicle (saline) was administered intraperitoneally, after which noxious rotations were conducted every 10 min for 1 hour. The number of action potentials each rotation evoked was counted offline using Spike 2 software (Cambridge Electronic Design), and the percent change in afferent firing was calculated. The conduction velocity of recorded joint afferents was determined by electrically stimulating the receptive field (0.6 Hz, 2-ms pulse width, 1 to 15 V) and dividing the latency of firing by the distance between the stimulating and recording electrodes.

RiboTag mice and quantitative reverse transcription polymerase chain reaction

To develop microglia (CX_3CR_1)–specific RiboTag mice, we crossed female homozygote RiboTag (*Rpl22*^{HA}) (stock #011029, The Jackson Laboratory) mice with male *Cx3cr1*-Cre^{ERT2} mice to generate *Cx3cr1*-Cre^{ERT2}::*Rpl22*^{HA}. At 3 weeks of age, the offspring received an intraperitoneal injection of 1 mg of tamoxifen dissolved in sunflower oil for five consecutive days. The mice were used 28 days after the last tamoxifen injection to restrict the Cre-mediated recombination to microglia. RNA was isolated from the flash-frozen spinal cord tissue samples 7 days after MIA or saline injection samples. Briefly, the tissue was homogenized in a polysome buffer, and the supernatant from the lysate was incubated with 50 μl of anti–hemagglutinin (HA) magnetic beads (Miltenyi Biotec) for 2 hours at 4°C. Bead-bound RNA is recovered by a magnet, washed with a high-salt buffer three times, and purified using an RNeasy Micro kit (Qiagen) according to the manufacturer's instructions. RNA quantity was measured using NanoDrop1000 (Thermo Fisher Scientific). In a subset of experiments, RNA was isolated from flash-frozen L3-L5 DRGs of rats using the RNeasy Microkit (Qiagen) following the manufacturer's instructions and quantified with NanoDrop 1000 (Thermo Fisher Scientific). RNA was reversed-transcribed to complementary DNA using a QuantiTect reverse transcriptase kit (Qiagen). Transcript levels were assessed using SYBR Green PCR Master Mix (Bio-Rad) in Step One Plus RT-PCR System (Applied Biosciences). Fold enrichment was calculated using the $\Delta\Delta C_t$ method with normalization to glyceraldehyde-3-phosphate dehydrogenase (GAPDH) or 60S acidic ribosomal protein large P1 (RPLP). Primer sequences were as follows: IL-1β mouse, CCTGCAGCTGGAGAGTGTGGAT (forward) and TGTGCTCTGCTTGTGAGGTGCT (reverse); GAPDH, TCATGACCACAGTGGATGCC (forward) and GGAGTTGCTGTTGAAGTCGC (reverse); Csf1 rat, GACGATCCCGTTTGCTACCTAA (forward) and GCGCATGGTTTCCTCGATT (reverse); RPLP rat, TACCTGCTCAGAACACCGGTCT (forward) and GCACATCGCTCAGGATTTCAA (reverse).

BV2 cells and IL-1β ELISA detection

BV2 microglia-like cells were maintained in DMEM (Gibco) containing 5% FBS and 1% penicillin-streptomycin at 37°C with 5% CO_2. BV2 cells were harvested from a 100-mm dish using a cell scraper, collected in 500 μl, and equally aliquoted into Eppendorf tubes before treatment. Cells were stimulated with 300 μM BzATP (Tocris) in ECS for 30 min at 37°C. In a subset of experiments, cells were treated with 10 μM ^{10}panx or ^{scr}panx (New England Peptide) in ECS for 30 min at 37°C before BzATP stimulation. As a control, ECS alone was used in equivalent volumes to BzATP. Enzyme-linked immunosorbent assay (ELISA) kits for mouse and rat IL-1β (R&D Systems) were used for quantification of IL-1β in cell culture supernatants or spinal cord homogenates as per the manufacturer's instruction. The concentration of IL-1β was normalized to protein levels (BCA Assay, Life Technologies) for spinal cord homogenates.

Western blotting

Rats were anesthetized with pentobarbital (Bimeda-MTC Animal Health Inc.) and perfused transcardially with PBS. L3-L5 DRGs were rapidly isolated, pooled, and homogenized in a homogenization buffer containing 20 mM tris-HCl (pH 7.5), 0.5% Tween 20, and 150 mM NaCl. Samples were incubated on ice for 30 min and centrifuged for 20 min at 12,000 rpm at 4°C. Total protein was measured using the BCA Protein Assay Kit (Thermo Fisher Scientific). Samples were combined with a loading buffer (350 mM tris, 30% glycerol, 1.6% SDS, 1.2% bromophenol blue, 6% β-mercaptoethanol) and heated for 10 min at 95°C before electrophoreses on a precast SDS gel (4 to 12% tris-HCl, Bio-Rad). Gels were transferred onto nitrocellulose membrane and probed with goat anti-Csf1 antibody (1:1000, AF416, R&D Systems) and mouse anti–β-actin (1:2000, A5316, Sigma). Membranes were washed in TBST (20 mM tris, 137 mM NaCl, and 0.05% Tween 20) and incubated for 1 hour at room temperature with anti-goat and anti-mouse conjugated IR dye (1:5000, Mandel Scientific) secondary antibodies. Membranes were then imaged using the Licor Odyssey C1x Infrared Imaging System (Mandel Scientific), and band intensity was quantified using ImageJ with normalization to β-actin.

Rat DRG immunohistochemistry

Rats were anesthetized with pentobarbital and perfused transcardially with PBS and then 10% NBF. Rat L3-L5 DRGs were dissected 7 days after intra-articular MIA or saline injection and postfixed for 1 day in 10% NBF. After fixation, the DRGs were embedded in paraffin using Leica Automatic Tissue Processor. Rat DRG sections were cut at 10 μm on a microtome (Leica) directly on slide and stained with rabbit anti-ATF3 (1:500, NBP 185816, Novus Biologicals) overnight at 4°C. Slides were washed in PBS and stained with conjugated donkey anti-rabbit IgG Cy5 (1:500, Jackson ImmunoResearch). Images were obtained using a Nikon A1R multiphoton microscope. The images were converted using NIS-Elements imaging software (Nikon), and counting of ATF3-positive cells was performed using ImageJ (NIH).

ACL transection

C57BL6/J male mice (12 weeks of age) and *Cx3cr1*-Cre^{ERT2}::*Panx1*$^{flx/flx}$ mice (8 weeks of age) treated with tamoxifen or vehicle were anesthetized with isoflurane (2 to 5% in 100% oxygen) inhalation anesthetic, with postoperative pain control provided (buprenorphine, 0.05 mg/kg intraperitoneally) on the day of surgery. The hindlimb area was shaved and disinfected, and sterile surgical drapes were applied. Under magnification (Leica M320 surgical microscope), the left knee joint was exposed through an anterior skin incision, the joint was opened by a medial parapatellar capsulotomy, the patella was dislocated laterally and then with the knee in full flexion, and the ACL was identified and transected with microscissors (ACLx) (*21*). The patella was repositioned, and the joint capsule was sutured with 7-0 nylon suture. Sham mice were treated in the same manner but without ACLx. Mechanical paw withdrawal threshold was assessed using the von Frey filament

test: Behavioral tests were performed weekly after ACLx. At week 13, a single intraperitoneal injection of probenecid (100 mg/kg intraperitoneally) or saline was administered, and mechanical threshold was assessed at 1, 2, 4, and 6 hours after injection.

SUPPLEMENTARY MATERIALS

Supplementary material for this article is available at http://advances.sciencemag.org/cgi/content/full/4/8/eaas9846/DC1

Fig. S1. MIA induces mechanical allodynia in rats.

Fig. S2. ATF3 and CSF1 expression in L3-L5 DRG is comparable in sham and MIA joint-injured rats on day 7.

Fig. S3. Microglial proliferation and Mac1-saporin depletion of spinal microglia.

Fig. S4. Characterization of microglial Panx1-deficient mice.

Fig. S5. Dynamic weight-bearing baseline quantification.

Fig. S6. Probenecid does not alter primary joint afferent activity.

Fig. S7. Probenecid alleviates ACLx-induced joint pain.

REFERENCES AND NOTES

1. M. T. Hannan, D. T. Felson, T. Pincus, Analysis of the discordance between radiographic changes and knee pain in osteoarthritis of the knee. *J. Rheumatol.* **27**, 1513–1517 (2000).
2. S. E. Gwilym, J. R. Keltner, C. E. Warnaby, A. J. Carr, B. Chizh, I. Chessell, I. Tracey, Psychophysical and functional imaging evidence supporting the presence of central sensitization in a cohort of osteoarthritis patients. *Arthritis Rheum.* **61**, 1226–1234 (2009).
3. D. R. Sagar, J. J. Burston, G. J. Hathway, S. G. Woodhams, R. G. Pearson, A. J. Bennett, D. A. Kendall, B. E. Scammell, V. Chapman, D. R. Sagar, J. J. Burston, G. J. Hathway, S. G. Woodhams, R. G. Pearson, A. J. Bennett, D. A. Kendall, B. E. Scammell, V. Chapman, The contribution of spinal glial cells to chronic pain behaviour in the monosodium iodoacetate model of osteoarthritic pain. *Mol. Pain* **7**, 88 (2011).
4. F. R. Nieto, A. K. Clark, J. Grist, V. Chapman, M. Malcangio, Calcitonin gene-related peptide-expressing sensory neurons and spinal microglial reactivity contribute to pain states in collagen-induced arthritis. *Arthritis Rheumatol.* **67**, 1668–1677 (2015).
5. W. Rahman, R. Patel, A. H. Dickenson, Electrophysiological evidence for voltage-gated calcium channel 2 (Ca_v2) modulation of mechano- and thermosensitive spinal neuronal responses in a rat model of osteoarthritis. *Neuroscience* **305**, 76–85 (2015).
6. T. Pitcher, J. Sousa-Valente, M. Malcangio, The monoiodoacetate model of osteoarthritis pain in the mouse. *J. Vis. Exp.* 53746 (2016).
7. D. B. Bas, J. Su, G. Wigerblad, C. I. Svensson, Pain in rheumatoid arthritis: Models and mechanisms. *Pain Manag.* **6**, 265–284 (2016).
8. J. A. Hendiani, K. N. Westlund, N. Lawand, N. Goel, J. Lisse, T. McNearney, Mechanical sensation and pain thresholds in patients with chronic arthropathies. *J. Pain* **4**, 203–211 (2003).
9. A. Surprenant, F. Rassendren, E. Kawashima, R. A. North, G. Buell, The cytolytic P_{2Z} receptor for extracellular ATP identified as a P_{2X} receptor (P2X7). *Science* **272**, 735–738 (1996).
10. P. Pelegrin, A. Surprenant, Pannexin-1 mediates large pore formation and interleukin-1β release by the ATP-gated P2X7 receptor. *EMBO J.* **25**, 5071–5082 (2006).
11. D. Bravo, P. Ibarra, J. Retamal, T. Pelissier, C. Laurido, A. Hernandez, L. Constandil, Pannexin 1: A novel participant in neuropathic pain signaling in the rat spinal cord. *Pain* **155**, 2108–2115 (2014).
12. J. L. Weaver, S. Arandjelovic, G. Brown, S. K. Mendu, M. S. Schappe, M. W. Buckley, Y.-H. Chiu, S. Shu, J. K. Kim, J. Chung, J. Krupa, V. Jevtovic-Todorovic, B. N. Desai, K. S. Ravichandran, D. A. Bayliss, Hematopoietic pannexin 1 function is critical for neuropathic pain. *Sci. Rep.* **7**, 42550 (2017).
13. T. Masuda, Y. Ozono, S. Mikuriya, Y. Kohro, H. Tozaki-Saitoh, K. Iwatsuki, H. Uneyama, R. Ichikawa, M. W. Salter, M. Tsuda, K. Inoue, Dorsal horn neurons release extracellular ATP in a VNUT-dependent manner that underlies neuropathic pain. *Nat. Commun.* **7**, 12529 (2016).
14. N. E. Burma, R. P. Bonin, H. Leduc-Pessah, C. Baimel, Z. F. Cairncross, M. Mousseau, J. V. Shankara, P. L. Stemkowski, D. Baimoukhametova, J. S. Bains, M. C. Antle, G. W. Zamponi, C. M. Cahill, S. L. Borgland, Y. De Koninck, T. Trang, Blocking microglial pannexin-1 channels alleviates morphine withdrawal in rodents. *Nat. Med.* **23**, 355–360 (2017).
15. C. N. Parkhurst, G. Yang, I. Ninan, J. N. Savas, J. R. Yates III, J. J. Lafaille, B. L. Hempstead, D. R. Littman, W.-B. Gan, Microglia promote learning-dependent synapse formation through brain-derived neurotrophic factor. *Cell* **155**, 1596–1609 (2013).
16. L. Constandil, A. Hernández, T. Pelissier, O. Arriagada, K. Espinoza, H. Burgos, C. Laurido, Effect of interleukin-1β on spinal cord nociceptive transmission of normal and monoarthritic rats after disruption of glial function. *Arthritis Res. Ther.* **11**, R105 (2009).
17. K. Y. Lee, S. A. Prescott, Chloride dysregulation and inhibitory receptor blockade yield equivalent disinhibition of spinal neurons yet are differentially reversed by carbonic anhydrase blockade. *Pain* **156**, 2431–2437 (2015).
18. S. L. Gustafson-Vickers, V. B. Lu, A. Y. Lai, K. G. Todd, K. Ballanyi, P. A. Smith, Long-term actions of interleukin-1β on delay and tonic firing neurons in rat superficial dorsal horn and their relevance to central sensitization. *Mol. Pain* **4**, 63 (2008).
19. A. J. Reeve, S. Patel, A. Fox, K. Walker, L. Urban, Intrathecally administered endotoxin or cytokines produce allodynia, hyperalgesia and changes in spinal cord neuronal responses to nociceptive stimuli in the rat. *Eur. J. Pain* **4**, 247–257 (2000).
20. W. Silverman, S. Locovei, G. Dahl, Probenecid, a gout remedy, inhibits pannexin 1 channels. *Am. J. Physiol. Cell Physiol.* **295**, C761–C767 (2008).
21. J. A. Beye, D. A. Hart, R. C. Bray, J. J. McDougall, P. T. Salo, Injury-induced changes in mRNA levels differ widely between anterior cruciate ligament and medial collateral ligament. *Am. J. Sports Med.* **36**, 1337–1346 (2008).
22. E. Teeple, G. D. Jay, K. A. Elsaid, B. C. Fleming, Animal models of osteoarthritis: Challenges of model selection and analysis. *AAPS J.* **15**, 438–446 (2013).
23. P. T. Salo, E. Theriault, Number, distribution and neuropeptide content of rat knee joint afferents. *J. Anat.* **190** (Pt. 4), 515–522 (1997).
24. N. Schuelert, J. J. McDougall, Grading of monosodium iodoacetate-induced osteoarthritis reveals a concentration-dependent sensitization of nociceptors in the knee joint of the rat. *Neurosci. Lett.* **465**, 184–188 (2009).
25. A. Bhattacharya, K. Biber, The microglial ATP-gated ion channel P2X7 as a CNS drug target. *Glia* **64**, 1772–1787 (2016).
26. E. C. Keystone, M. M. Wang, M. Layton, S. Hollis, I. B. McInnes; D1520C00001 Study Team, Clinical evaluation of the efficacy of the P2X7 purinergic receptor antagonist AZD9056 on the signs and symptoms of rheumatoid arthritis in patients with active disease despite treatment with methotrexate or sulphasalazine. *Ann. Rheum. Dis.* **71**, 1630–1635 (2012).
27. N. Arulkumaran, R. J. Unwin, F. W. Tam, A potential therapeutic role for P2X7 receptor (P2X7R) antagonists in the treatment of inflammatory diseases. *Expert Opin. Invetig. Drugs* **20**, 897–915 (2011).
28. V. L. Harvey, A. H. Dickenson, Behavioural and electrophysiological characterisation of experimentally induced osteoarthritis and neuropathy in C57Bl/6 mice. *Mol. Pain* **5**, 18 (2009).
29. J. A. M. Coull, D. Boudreau, K. Bachand, S. A. Prescott, F. Nault, A. Sík, P. De Koninck, Y. De Koninck, Trans-synaptic shift in anion gradient in spinal lamina I neurons as a mechanism of neuropathic pain. *Nature* **424**, 938–942 (2003).
30. Y. Huang, J. B. Grinspan, C. K. Abrams, S. S. Scherer, Pannexin1 is expressed by neurons and glia but does not form functional gap junctions. *Glia* **55**, 46–56 (2007).
31. B. Ajami, J. L. Bennett, C. Krieger, W. Tetzlaff, F. M. V. Rossi, Local self-renewal can sustain CNS microglia maintenance and function throughout adult life. *Nat. Neurosci.* **10**, 1538–1543 (2007).
32. R. van Furth, Z. A. Cohn, The origin and kinetics of mononuclear phagocytes. *J. Exp. Med.* **128**, 415–435 (1968).
33. J. Lampa, M. Westman, D. Kadetoff, A. N. Agréus, E. Le Maître, C. Gillis-Haegerstrand, M. Andersson, M. Khademi, M. Corr, C. A. Christianson, A. Delaney, T. L. Yaksh, E. Kosek, C. I. Svensson, Peripheral inflammatory disease associated with centrally activated IL-1 system in humans and mice. *Proc. Natl. Acad. Sci. U.S.A.* **109**, 12728–12733 (2012).
34. P. M. Fiorentino, R. H. Tallents, J. N. Miller, S. M. Brouxhon, M. K. O'Banion, J. E. Puzas, S. Kyrkanides, Spinal interleukin-1β in a mouse model of arthritis and joint pain. *Arthritis Rheum.* **58**, 3100–3109 (2008).
35. W. A. Banks, A. J. Kastin, R. D. Broadwell, Passage of cytokines across the blood-brain barrier. *Neuroimmunomodulation* **2**, 241–248 (1995).
36. A. K. Clark, R. Wodarski, F. Guida, O. Sasso, M. Malcangio, Cathepsin S release from primary cultured microglia is regulated by the P2X7 receptor. *Glia* **58**, 1710–1726 (2010).
37. K. L. Hyrich, D. P. M. Symmons, K. D. Watson, A. J. Silman; British Society for Rheumatology Biologics Register, Comparison of the response to infliximab or etanercept monotherapy with the response to cotherapy with methotrexate or another disease-modifying antirheumatic drug in patients with rheumatoid arthritis: Results from the British Society for Rheumatology Biologics Register. *Arthritis Rheum.* **54**, 1786–1794 (2006).
38. R. Bartlett, L. Stokes, S. J. Curtis, B. L. Curtis, R. Sluyter, Probenecid directly impairs activation of the canine P2X7 receptor. *Nucleosides Nucleotides Nucleic Acids* **36**, 736–744 (2017).
39. K. Kanjanamekanant, P. Luckprom, P. Pavasant, P2X7 receptor–Pannexin1 interaction mediates stress-induced interleukin-1 beta expression in human periodontal ligament cells. *J. Periodontal Res.* **49**, 595–602 (2014).
40. H. F. Cserr, D. H. VanDyke, 5-Hydroxyindoleacetic acid accumulation by isolated choroid plexus. *Am. J. Physiol.* **220**, 718–723 (1971).
41. A. Bhattacharya, Q. Wang, H. Ao, J. R. Shoblock, B. Lord, L. Aluisio, I. Fraser, D. Nepomuceno, R. A. Neff, N. Welty, T. W. Lovenberg, P. Bonaventure, A. D. Wickenden,

M. A. Letavic, Pharmacological characterization of a novel centrally permeable P2X7 receptor antagonist: JNJ-47965567. *Br. J. Pharmacol.* **170**, 624–640 (2013).
42. G. M. Pitcher, J. Ritchie, J. L. Henry, Paw withdrawal threshold in the von Frey hair test is influenced by the surface on which the rat stands. *J. Neurosci. Methods* **87**, 185–193 (1999).
43. R. P. Bonin, C. Bories, Y. De Koninck, A simplified up-down method (SUDO) for measuring mechanical nociception in rodents using von Frey filaments. *Mol. Pain* **10**, 26 (2014).
44. B. D. Bomsta, L. C. Bridgewater, R. E. Seegmiller, Premature osteoarthritis in the Disproportionate micromelia (*Dmm*) mouse. *Osteoarthritis Cartilage* **14**, 477–485 (2006).
45. K. P. H. Pritzker, S. Gay, S. A. Jimenez, K. Ostergaard, J. P. Pelletier, P. A. Revell, D. Salter, W. B. van den Berg, Osteoarthritis cartilage histopathology: Grading and staging. *Osteoarthritis Cartilage* **14**, 13–29 (2006).
46. K. Ichikizaki, S. Toya, T. Hoshino, A new procedure for lumbar puncture in the mouse (intrathecal injection) preliminary report. *Keio J. Med.* **28**, 165–171 (1979).
47. C. C. Pegg, C. He, A. R. Stroink, K. A. Kattner, C. X. Wang, Technique for collection of cerebrospinal fluid from the cisterna magna in rat. *J. Neurosci. Methods* **187**, 8–12 (2010).
48. N. L. Weilinger, P. L. Tang, R. J. Thompson, Anoxia-induced NMDA receptor activation opens pannexin channels via Src family kinases. *J. Neurosci.* **32**, 12579–12588 (2012).

Acknowledgments: We thank D. Littman and W.-B. Gan (both at New York University School of Medicine) for providing *Cx3cr1*-Cre^{ERT2} mice, R. Thompson (University of Calgary) for *Panx1*$^{flx/flx}$ mice, and D. Ponjevic for joint histology. **Funding:** This work was supported by grants from the Rita Allen Foundation and American Pain Society, Vi Riddell Program for Pediatric Pain, and Natural Sciences and Engineering Research Council of Canada (RGPIN418299) to T.T. Canadian Institutes of Health Research grants were awarded to T.T. (MOP133523), S.A.P. (PJT-153161), J.J.M. (PJCT-153303), and G.W.Z. (FDN143336). N.E.B., H.L.-P., and M.M. are supported by Alberta Innovates Studentships. **Author contributions:** M.M. and T.T. conceived and designed the project. M.M., N.E.B., K.Y.L., H.L.-P., A.R.R., M.O., C.H.T.K., B.S., N.P., P.S., and P.L.S. performed the experiments. T.T., J.R.M., J.A.S., J.B., G.W.Z., S.A.P., and J.J.M. supervised the experiments. M.M., N.E.B., H.L.-P., K.Y.L., A.R.R., and M.O. analyzed the data. M.M., C.H.T.K., and T.T. wrote the manuscript. **Competing interests:** The authors declare that they have no competing interests. **Data and materials availability:** All data needed to evaluate the conclusions in the paper are present in the paper and/or the Supplementary Materials. Additional data related to this paper may be requested from the authors.

Submitted 22 January 2018
Accepted 26 June 2018
Published 8 August 2018
10.1126/sciadv.aas9846

Citation: M. Mousseau, N. E. Burma, K. Y. Lee, H. Leduc-Pessah, C. H. T. Kwok, A. R. Reid, M. O'Brien, B. Sagalajev, J. A. Stratton, N. Patrick, P. L. Stemkowski, J. Biernaskie, G. W. Zamponi, P. Salo, J. J. McDougall, S. A. Prescott, J. R. Matyas, T. Trang, Microglial pannexin-1 channel activation is a spinal determinant of joint pain. *Sci. Adv.* **4**, eaas9846 (2018).